Electromiographic Signal Processing Using Embedded Artificial Intelligence: An Adaptive Filtering Approach

Daniel Proaño-Guevara[1]*, Xiomara Blanco Valencia[2], Paul D. Rosero-Montalvo[3], Diego H. Peluffo-Ordóñez[4,5]*

[1] Instituto Superior Técnico – Universidade de Lisboa, (Portugal)
[2] Universidad Internacional de La Rioja, Logroño (Spain)
[3] Computer Science department, IT University of Copenhagen, (Denmark)
[4] Modeling, Simulation and Data Analysis (MSDA) Research Program, Mohammed VI Polytechnic University, (Morocco)
[5] Faculty of Engineering, Corporación Universitaria Autónoma de Nariño, Pasto, (Colombia)

Received 26 July 2022 | Accepted 9 August 2022 | Published 18 August 2022

Abstract

In recent times, Artificial Intelligence (AI) has become ubiquitous in technological fields, mainly due to its ability to perform computations in distributed systems or the cloud. Nevertheless, for some applications -as the case of EMG signal processing- it may be highly advisable or even mandatory an on-the-edge processing, i.e., an embedded processing methodology. On the other hand, sEMG signals have been traditionally processed using LTI techniques for simplicity in computing. However, making this strong assumption leads to information loss and spurious results. Considering the current advances in silicon technology and increasing computer power, it is possible to process these biosignals with AI-based techniques correctly. This paper presents an embedded-processing-based adaptive filtering system (here termed edge AI) being an outstanding alternative in contrast to a sensor-computer- actuator system and a classical digital signal processor (DSP) device. Specifically, a PYNQ-Z1 embedded system is used. For experimental purposes, three methodologies on similar processing scenarios are compared. The results show that the edge AI methodology is superior to benchmark approaches by reducing the processing time compared to classical DSPs and general standards while maintaining the signal integrity and processing it, considering that the EMG system is not LTI. Likewise, due to the nature of the proposed architecture, handling information exhibits no leakages. Findings suggest that edge computing is suitable for EMG signal processing when an on-device analysis is required.

Keywords

Adaptive Filters, Artificial Intelligence On-The-Edge (Edge AI), Digital Signal Processor (DSP), Electromyography (EMG), Embedded Processing, Intelligent Processing, Online Processing.

DOI: 10.9781/ijimai.2022.08.009

I. Introduction

Biomedical signal processing and proper filtering are critical for designing intelligent prosthesis, neurorehabilitation, and clinical diagnosis [1], [2]. In this regard, assisting people with physical disabilities is one of the main concerns, as it directly impacts activities of daily living (ADLs) and thus the quality of life [3]–[8]. The electromyogram (EMG) is one of the most studied biosignals in the medical and engineering fields [9]. EMG signals are generated by physiological variations in the state of the muscle fiber membranes, i.e., muscle contractions [10]–[12]. Electromyography is a technique for evaluating the generation, recording, and analyzing of muscle signals [11], [13]. Therefore, it is necessary to understand how EMG evaluates muscle activation to process and interpret it correctly [14]. EMG signals are compound biomedical signals because they are generated by a spatiotemporal interferential summation of action potentials [1], [15]. Thus, EMG is considered a pseudo-stochastic, non-stationary, linear signal [1], [14], [15], with a time-varying or dynamic model being the most suitable approach to analyze it [16].

There are two main types of EMG analysis [11]: neurological and kinesiological. On the one hand, the neurological analysis evaluates the response of a muscle to external electrical stimulation under static conditions. On the other hand, the kinesiological analysis evaluates neuromuscular activation during voluntary movements. For example, kinesiological protocols may assess muscle activity during postural tasks and functional exercises under a rehabilitation or training program.

According to the type of electrodes used for signal recording, there are two kinds of EMG: intramuscular EMG and surface EMG. Intramuscular EMG is an invasive technique that uses a monopolar needle electrode to detect a subject's motor unit potential (MUP). Meanwhile, surface EMG records muscle activity using at least a pair of electrodes on the skin surface. The latter method is the most commonly used to monitor voluntary contractions for kinesiological studies [12], [13]. Finally, EMG is also classified according to the topographic anatomical location of the muscle group being analyzed [13], [17].

* Corresponding author.
E-mail addresses: daniel.proano@sdas-group.com (D. Proaño), diego.peluffo@sdas-group.com (D. Peluffo).

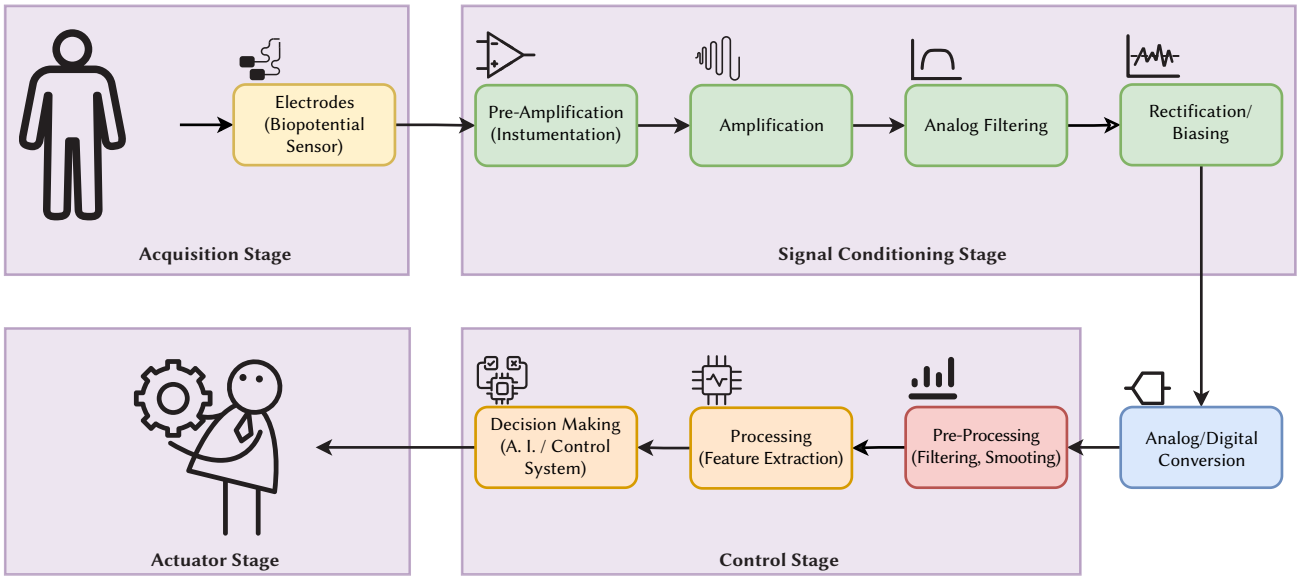

Fig. 1. Biopotential sensing and processing stages.

Kinesiological surface electromyography (KSEMG) is widely used as a **study and evaluation tool** [11] for biomechanics [18], diagnosis [19], [20], rehabilitation research [21], user-prosthesis interfaces [9], [12], [22] and human-machine interfaces for several devices [23]. Thus, this study focuses on the KSEMG analysis.

As a result of several groups standardizing EMG signal acquisition processes [24], the SENIAM project (Surface Electromyography for Non-Invasive Assessment of Muscles) began in 1996 to formulate recommendations for studying EMG signals. These recommendations include information on sensor types and location, signal processing, and characteristic curve modeling [24], [25]. Regarding biopotential sensing systems, the main stages are the power supply, pre-amplification with an instrumentation amplifier, analog filtering, rectification, analog-digital conversion, and control [11], [25]–[27].

Raw EMG signals typically vary between a few microvolts and 2-3 millivolts. Therefore, this signal is usually amplified by a minimum gain of 500 with preamplifiers, extending to 1000 when using units with passive leads. Differential amplifiers are used at this stage, allowing differential signals and rejecting common-mode voltages between input terminals and common ground [11], [13]. The frequency range of the EMG signal is between 10Hz to 500Hz [12], [20]. It is recommended to avoid any notch filter as it destroys too much information [11]. The rectification stage reflects all the signals below the baseline average. Rectification facilitates the reading and computational analysis of the data. In the control stage, digital signal processing (DSP) is widely applied in techniques such as signal smoothing, amplitude normalization of the acquired signal, and removal of artifacts. [25], [27]–[30].

For more complex applications, as with prosthetic devices, the control stage is subdivided into different stages: signal filtering and smoothing are the pre-processing components, and feature extraction is the processing step. Later, a classification stage [12], [22], which will be called the decision-making stage in this article, finally passes to an actuating stage [9], [19],[21]–[23].

Fig. 1 shows the biopotential sensing and processing stages and sub-stages. This paper focuses on the pre-processing block, highlighted in red, specifically in the digital filtering of KSEM signals.

Digital signal processing (DSP) is a branch of computer science specializing in a single type of data, signals [31]. DSP consists of mathematics, algorithms, and techniques related to representing, transforming, and manipulating signals and their information after digitization [31], [32]. Unlike the signal processing techniques of analog electronics, DSP techniques guarantee reproducibility and accuracy of results, recognizing them as superior and more reliable in certain circumstances than their analog counterparts [33].

Intelligent signal processing (ISP) uses machine learning and other 'smart' techniques to extract as much information as possible from the received signal data -in the case of EMG signals, information can be extracted through proper characterization stages as studied in [34], [35]. Classical signal processing methods are robust and straightforward tools that work incomparably with mathematical models that are linear, stationary, and Gaussian. However, real systems are non-linear, with erratic or impulsive statistical structures that can vary over time. Minimal signal or noise-structure changes can lead to qualitative changes in how classical processing systems filter noise or maintain stability [36]. Adaptive filtering is an *Online Learning* technique. It trains its parameters while acquiring information, unlike machine learning which usually trains on the entire dataset or at least a mini-batch of data. Adaptive filtering can be considered an Artificial Intelligence technique since it seeks to minimize an error signal using stochastic gradient descent (SGD) and falls into the field of 'Computer Perception.' It has become one of the most efficient methods for acquiring physiological signals [37]. One approach for denoising is the adaptive noise cancellation of EMG signals, which uses an external noise source loosely related to the noise implicit in the EMG signal. For this task, filtering algorithms such as Kalman Filter, LMS (Least Mean Squares), RLS (Recursive-Least-Squares), Wiener, UFIR (Finite Impulse Response), Gaussian, bee colony algorithms, and Bayesian, among others, have been implemented [38]–[44].

The RLS filtering algorithm seeks to minimize the sum of squares of the differences between the desired signal and the filter output, updating iteratively as new information is acquired. This algorithm solves least squares estimation recursively [43], [45]–[48]. Few works have been found on edge intelligent EMG signal processing (on the embedded system). Diniz and Limem [45], [46] perform traditional digital acquisition and filtering processes using a general-purpose GPU 'NVidia Jetson' as a shared device. They implement machine learning and decision-making algorithms, but there is no evidence of intelligent signal processing per se.

The scientific community is focused on pattern recognition and classification in prosthetic devices and recognizes that the variability in acquired SEMG signals between test subjects is significant [3], [6],

[49], [50]. Furthermore, the literature review has shown that the digital signal processing techniques used on EMG in embedded systems are for LTI systems [1], [14], [27]–[30],[51], [52]. Since EMG signals are pseudo-stochastic (therefore time-varying), these techniques are not the most suitable.

Therefore, using adaptive filtering algorithms in an embedded system to eliminate noise in sEMG signals is proposed as a scalable system for multiple users, reducing the time and complexity of system calibration. This approach respects the non-linear characteristics of the biologically-originated system preserving the information without substantial distortion and adaptability to a varying noise source; besides, it allows the filtering system to be used in multiple applications without significant modifications. This paper introduces an adaptive filtering system implemented on an embedded system (Edge AI) that uses a simulated white noise source as the target signal to be removed. To contrast and validate the model, an FIR filter is also implemented using classical DSP techniques (LTI) and the same adaptive filtering system but implemented in a sensor-computer-actuator system.

The results show that the embedded processing system achieves a similar filtering quality and performance as the sensor-computer-actuator system. Some of the essential advantages of the embedded system are eliminating any networking interfaces, guaranteeing the security of the acquired data, no latency, and no loss of communication between the computing device and the sensors and actuators.

The rest of this manuscript is organized as follows: Section II shows the hardware and the comparison approach used to validate the presented approach. Afterward, section III details the dataset used, the performance metrics, the benchmark methods and a comparison with previously published literature, and the experiment description that outlines the approaches used in this paper. Subsequently, section IV analyzes the results obtained in each of the benchmarks and the presented approach and discusses the authors' findings. Finally, section V concludes the article and draws ideas for further research.

II. Materials and Methods

A. Materials - Hardware & Testbench Architecture

The embedded system for processing is a PYNQ-Z1; it uses a ZYNQ-7000 SoC from XILINX composed of an ARM Cortex-A9 and programmable logic cells of the Artix-7 family. It works with a Linux-based operating system running Python notebooks as an interface medium.

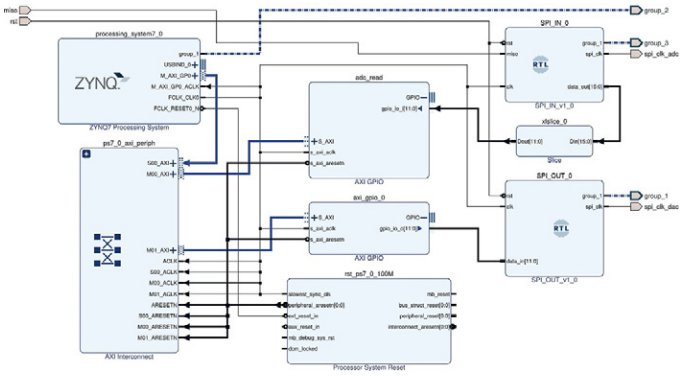

Fig. 2. Block diagram defining the behavior of the acquisition system.

On the one hand, the system incorporates a Digilent's PMOD AD1 module as a signal reading system, incorporating an AD7476 analog-to-digital converter (ADC). This converter has a maximum output rate of 1 MSPS at a resolution of 12 bits. On the other hand, the system uses a Digilent's PMOD DA2 module as a signal reconstruction system since it incorporates a DAC121S101 digital to analog converter (DAC). This converter has a maximum output rate of 1 MSPS at a resolution of 12 bits. Timing diagrams describe the communication of these systems. Thus, it is necessary to decode these protocols and implement them in HDL, using finite state machines (FSM) to model the required behaviors. All hardware blocks are linked together and interfaced with the ARM processor, completing the description of the real-time processing architecture. Fig. 2 shows the final result.

Digilent Analog Discovery 2's function generator recreates the EMG signals and is used to analyze the frequency and measure the parameters needed. The waveform's information comes from the public database [53], further described in A. Finally, Fig. 3 presents the architecture used in the experiment.

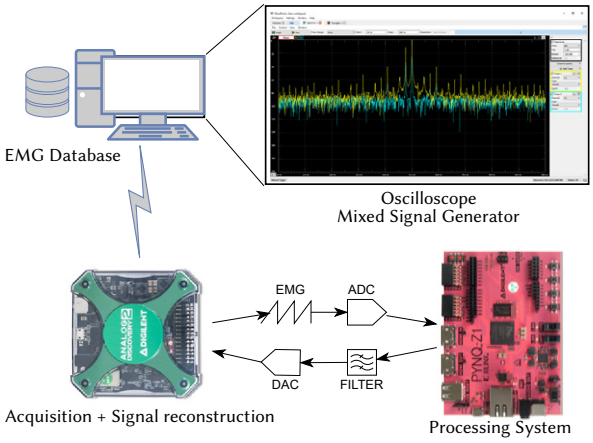

Fig. 3. Processing system architecture.

B. Comparison Approach

The test scenario of the three processing systems is designed based on the methodology presented in Fig. 4. The first scenario consists of a system architecture using classical DSP. In contrast, the second scenario consists of an embedded processing system, an adaptive RLS filter in a horizontal structure. Finally, scenario three involves processing using a sensor-computer-actuator system and wireless communication protocols. A common comparison framework for the three scenarios is set, where spectrograms, signal means, processing times, and SNR are analyzed.

The evaluation metrics for the test scenarios compare input and output signal averages, the time lag associated with the processing time, an analysis of the spectrogram, and the SNR of the signals. Finally, the evaluation metrics are contrasted between the three groups to determine the most suitable architecture for the EMG signal filtering tasks. The evaluation and testbench is further explained in B and C.

III. Experimental Setup

A. Dataset Description

The dataset "ISRMYO-I: A DATABASE FOR SEMG-BASED HAND GESTURE RECOGNITION" [53] consists of sEMG signals recorded for different hand gestures. The database follows an organization as raw EMG, the unprocessed recorded signals, and train and test, which are the relevant data to train a classifier model. This database recorded 16 channels of the forearm's sEMG with a multichannel sleeve sensor, firstly used for hand motion classification. The raw database was acquired with a sampling frequency of 1 kHz, and 12 Bits of resolution [54].

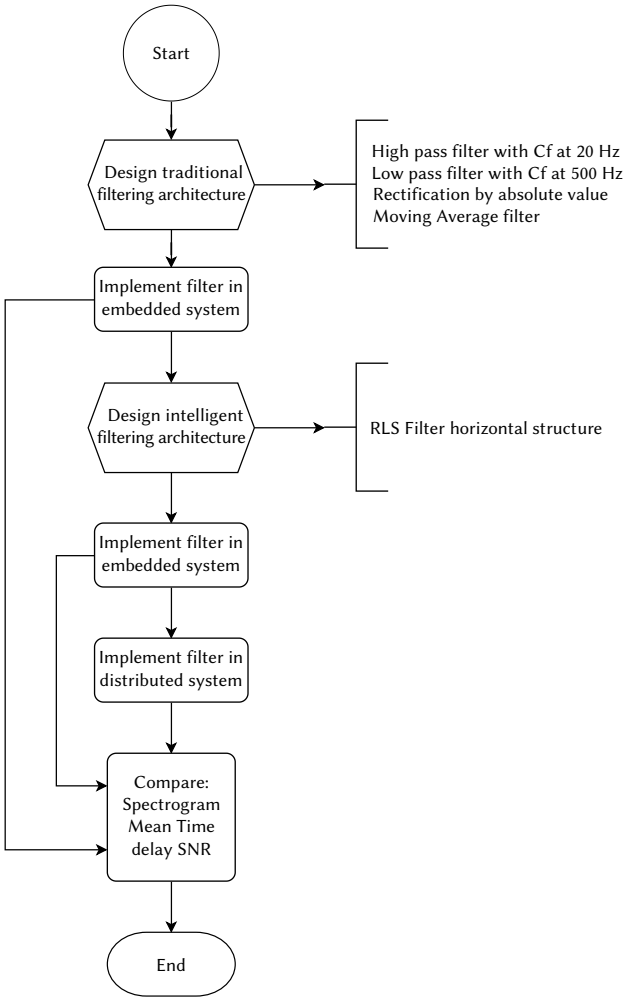

Fig. 4. Design and testing methodology for classical, intelligent embedded, and intelligent sensor-actuator-computer DSP processing paradigms.

The information used for reconstructing the sEMG signal comes from one subject. The maximum buffer memory (4096 points) for the arbitrary signal generator was selected to reconstruct the signal. The signal is then rescaled to 3 Vpp and a mean offset of 1.5 V.

B. Performance Metrics

One of the performance metrics used is the Signal-to-noise ratio SNR. According to [55] it is described as (1):

$$SNR = 10\log\left(\frac{\sum_{n=1}^{N} f(n)^2}{\sum_{n=1}^{N} [f(n) - \hat{f}(n)]^2}\right) \quad (1)$$

where, $f(n)$ is a signal containing noise, $\hat{f}(n)$ is the denoised signal, and N is the length of the signal.

The SNR compares the desired signal level to the noise level or the noisy signal. SNR is defined as the ratio of signal power to the noise power, and a ratio greater than 0 dB indicates more signal than noise.

Another metric used is the processing delay. It compares an inputted sinusoidal signal with the system's output and measures the time difference between the zero-crossing point of both signals.

C. Benchmark Methods

The benchmark methods considered for this work only analyze the filtering features.

The database authors [53] apply a DRMS (differential root mean square) processing to multiple channels. There is no single-channel processing and thus no possible benchmark comparations with this approach.

[56] states a resampling of the database to 1000 Hz and a band-pass filtering between 3 Hz to 300 Hz. No filtering architecture or metrics are presented.

[3] applies a 20-order 50 Hz comb filter to remove the power interference from the data. A db5 wavelet basis function of three layers threshold noise reduction is used, achieving an 8.8151 SNR.

Three different testbench scenarios are set to validate the proposed approach properly while taking the processing time, mean shifting, and SNR as a metric.

1. A classical DSP, where the embedded system performs all the computations, is set for the first comparison point with the characteristics taken from [27]:
   - A high-pass filter with a cutoff frequency of 20 Hz
   - Low-pass filter with a cutoff frequency of 500 Hz
   - Rectification with the sample absolute value
   - Smoothing through a moving average filter
2. The second approach is a real-time RLS filtering architecture with a sensor-computer-actuator paradigm. In this approach, the embedded system is used to acquire the sample, send it through Wi-Fi to a computer where it is filtered, and then wirelessly received and reconstructed.
3. The proposed approach, the one to be compared, eliminates the networking structure and external processing device to embed the computation.

D. Experiment Description

As described in the benchmark methods, the experimentation is composed of three tests, one implementing a classical DSP system and another as a sensor-computer-actuator system, where the sensor and the actuator communicate wirelessly with the computer through TCP-IP sockets, and finally, the embedded processing system.

The classical DSP processing system consists of a band-pass filter between 20 and 500 Hz in a horizontal FIR structure of 61 taps to facilitate the process and operation in real-time. The results of the FIR filter are then passed through an averaging filter with a window of 20 taps, from which its absolute value is previously obtained by way of rectification. This structure is implemented in the PYNQ embedded system.

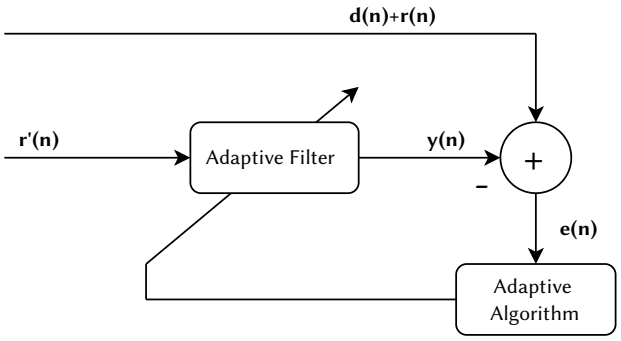

Fig. 5. Noise cancellation structure using adaptive filters.

The same filtering architecture is used for the sensor-computer-actuator system and the embedded AI processing system. A linear FIR and RLS filter structure is used, which will allow real-time learning of variations of the noise. Fig. 5 presents the adaptive noise cancellation structure. In this architecture, the input to the filter is the modeled signal or noise measurement $r'(n)$, and the desired signal

is the acquired signal (desired signal added with noise) $d(n) + r(n)$. Therefore, the filter's output would be the noise model, and the output $e(n)$ corresponds to the filtered signal. The model of the signal to be removed by the filtering structure is considered white noise. The simulation of a SEMG baseline, which would be the desired signal to be removed, is highly complicated because of the number of hyperparameters and is computationally expensive. Therefore, this model is avoided for online applications.

Fig. 6 shows the architecture of a horizontal RLS adaptive filter, which can process in real-time the acquired data, allowing online learning of the acquired data, thus adjusting to the circumstances in which the structure is being used. This architecture is similar to a neural unit of a perceptron since, in the forward step, it summates the multiplications of the inputs by their weights $\Sigma_k X(k) * W(k)$. Subsequently, it compares it with the desired signal $d(k)$ and generates an error signal $\epsilon(k)$. Finally, the error signal is backpropagated through the structure with an algorithm based on stochastic gradient descent (SGD).

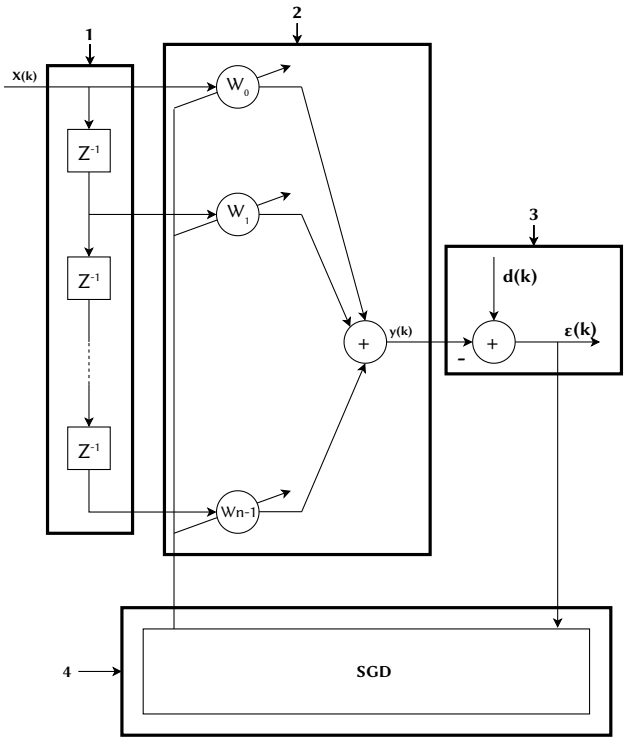

Fig. 6. Intelligent sEMG filtering algorithm for embedded processing. 1- Shows the delay taps of the filter, 2- presents the forward pass of the information, 3- corresponds to the error computation, and 4- is the SGD-based backpropagation algorithm.

IV. Results and Discussion

For the description of the results, the related tests and measurements will be presented, taking into account the signals in the same contextual frame, their spectrograms, and a propagation delay analysis analyzed with pure sinusoidal signals.

A. Results of Classical DSP

Fig. 7 and Fig. 8 show that the algorithm works as soon as it is started, without needing waiting times.

Fig. 9 shows the original signal, filtered by DSP, and the superposition of both signals in an acquisition period of 4 minutes, at a sampling frequency of 4 kHz.

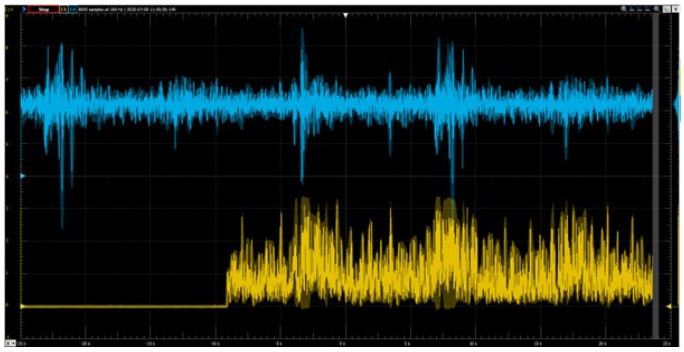

Fig. 7. Start of acquisition with traditional DSP, original signal [blue] and filtered signal [yellow], the horizontal axis represents time, while the vertical axis represents the amplitude in volts of the measured signal.

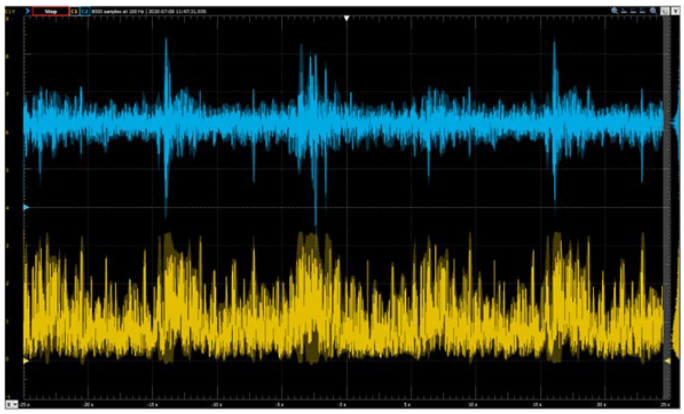

Fig. 8. Regular operation of traditional DSP, original signal (in blue) and filtered signal (in yellow), the horizontal axis represents time, while the vertical axis represents the amplitude in volts of the measured signal.

The visual analysis of the signals shows a radical change in the waveform, rectifying the impulses and leading it to oscillate from the 0 baseline without the additive component that moves the oscillation line, as in the original signal. The average of the original signal is 2.1908V, and the filtered signal is 0.9419V, which verifies what was described above. As for the spectra analysis, they can be observed in Fig. 10 and Fig. 11.

The high-frequency component of the signal is removed from the spectrograms, while the low-frequency component is distorted.

B. Results of Sensor-Computer-Actuator System

Fig. 12 and Fig. 13 show that the algorithm needs a minimum time to start working. Initially, the signal shows considerable noise, and it is impossible to identify the original signal, and after some time, it can be seen that the filtering effects are more noticeable, showing the adaptability of the filter.

Fig. 14 shows the original signal, filtered by the sensor-computer-actuator system, and the superposition of both signals in an acquisition period of 4 minutes, at a sampling frequency of 4kHz.

In addition, if a visual analysis is made, the signals appear similarly. The change is not radical given the noise source; the original signal's average is 2.193V, and the filtered signal is 2.175V, which shows that they maintain their characteristics to a large extent. It should be emphasized that in Fig. 20. errors are observed in the data communication reflected both in the wave's shape and information gaps in the spectrogram. The loss of information jeopardizes the integrity of the filtering process, as these are critical data that should not be lost.

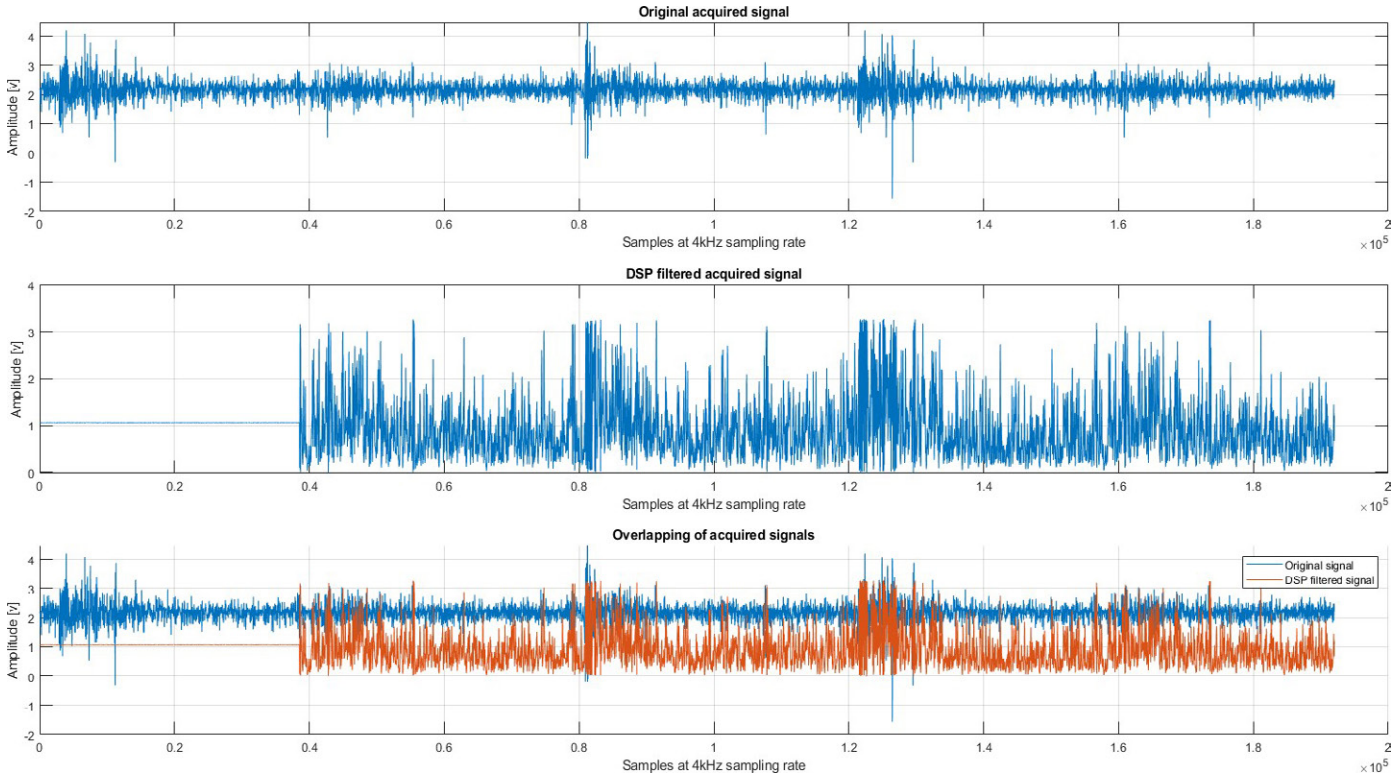

Fig. 9. Original signal vs filtered signal using traditional DSP.

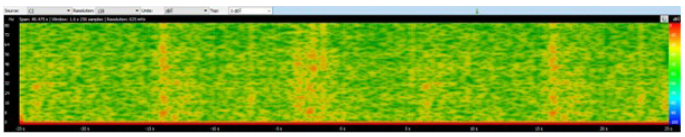

Fig. 10. Spectrogram of the original signal in a traditional DSP context. The horizontal axis represents time, while the vertical axis represents the frequency in Hz of the measured signal.

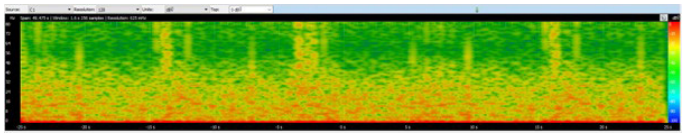

Fig. 11. Spectrogram of the filtered signal in a traditional DSP context. The horizontal axis represents time, while the vertical axis represents the frequency in Hz of the measured signal.

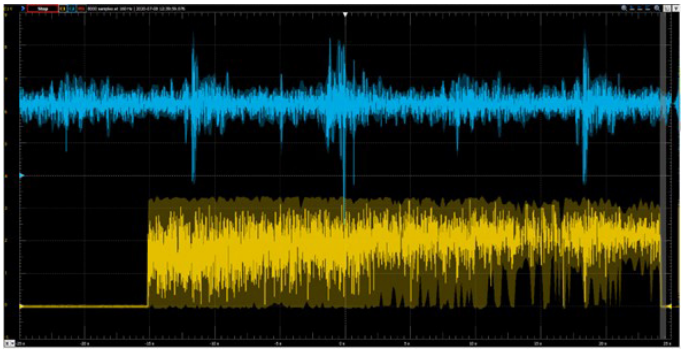

Fig. 12. Start of acquisition with the sensor-computer-actuator system: original signal [blue] and filtered signal [yellow]. The horizontal axis represents time, while the vertical axis represents the amplitude in volts of the measured signal.

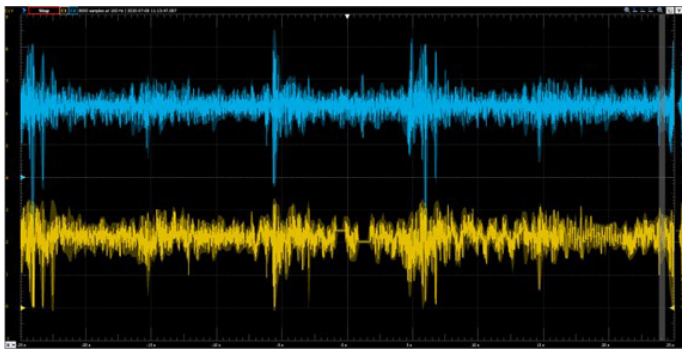

Fig. 13. Normal operation of the sensor-computer-actuator system: original signal [blue] and filtered signal [yellow]. The horizontal axis represents time, while the vertical axis represents the amplitude in volts of the measured signal.

The spectrogram analysis can be observed in Fig. 15 and Fig. 16.

No significant change can be seen comparing the spectrograms, except for the blurring effect in the impulsive peaks, regularizing the signal, and the concentration of the frequency components in the low bands.

C. Results of Embedded Processing

Fig. 17 and Fig. 18 show that the algorithm needs a minimum time to start working. Initially, the signal shows more noise than the original signal, and after some time, the filtering effects are more noticeable.

Fig. 19 shows the original signal, filtered by the on-the-edge system, and the superposition of both signals in an acquisition period of 4 minutes, at a sampling frequency of 4kHz.

The visual analysis of the signals shows that they maintain a remarkable similarity. The change is not radical, given the noise source. The average of the original signal is 2.192V, and the filtered signal is 2.173V, which shows that they maintain their characteristics.

As for the spectra analysis, they can be observed in Fig. 20 and Fig. 21.

The spectrogram comparison does not show much change, except for the blurring effect on the impulsive peaks, regularizing the signal.

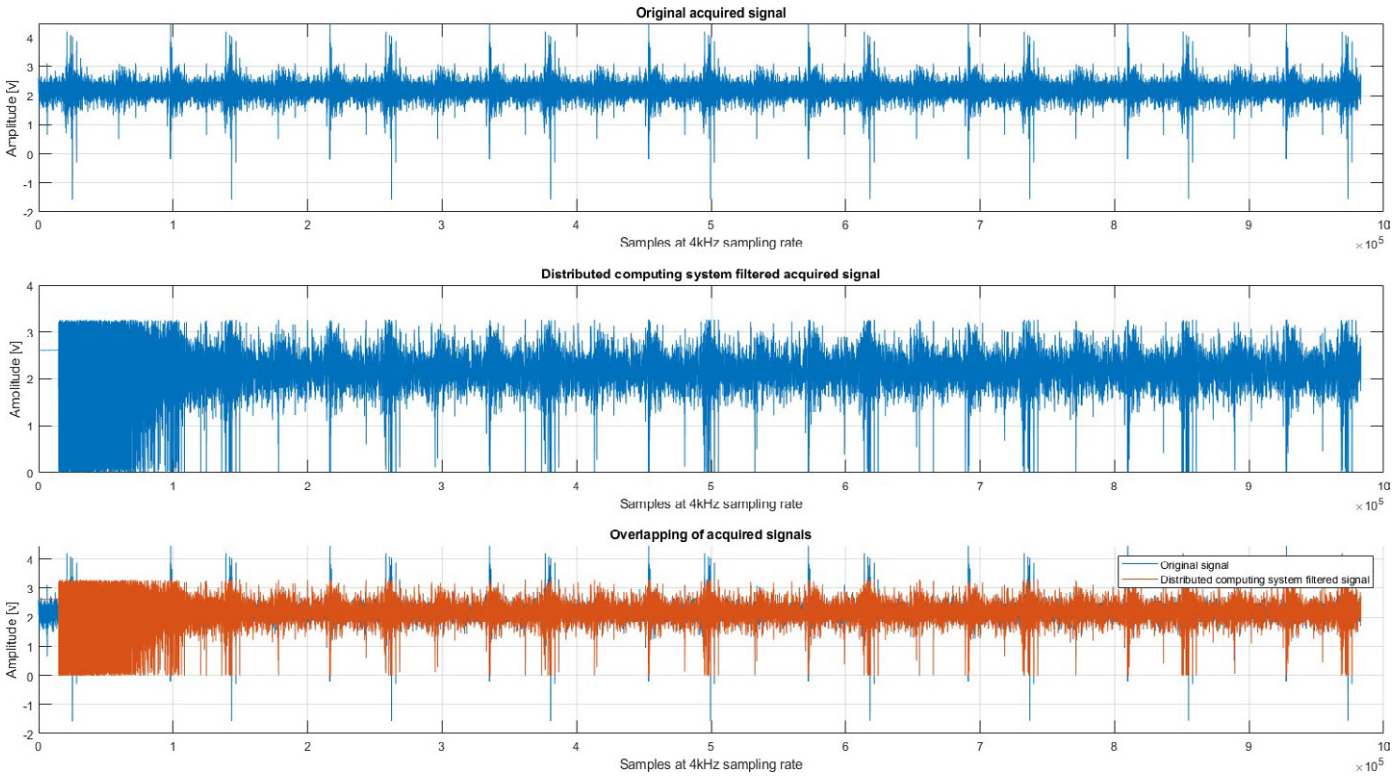

Fig. 14. Original signal vs filtered signal using the sensor-computer-actuator system.

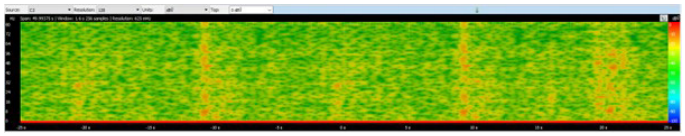

Fig. 15. Spectrogram of the original signal in the context of a distributed computing system. The horizontal axis represents time, while the vertical axis represents the frequency in Hz of the measured signal.

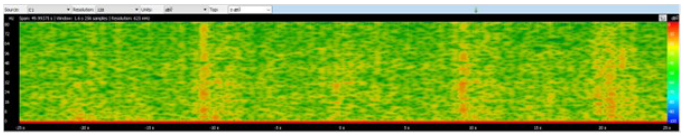

Fig. 16. Spectrogram of the filtered signal in the context of a distributed computing system. The horizontal axis represents time, while the vertical axis represents the frequency in Hz of the measured signal.

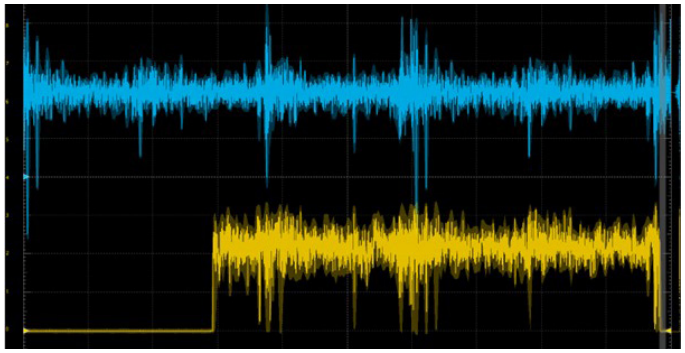

Fig. 17. Start of acquisition with embedded processing: original signal [blue] and filtered signal [yellow]. The horizontal axis represents time, while the vertical axis represents the amplitude in volts of the measured signal.

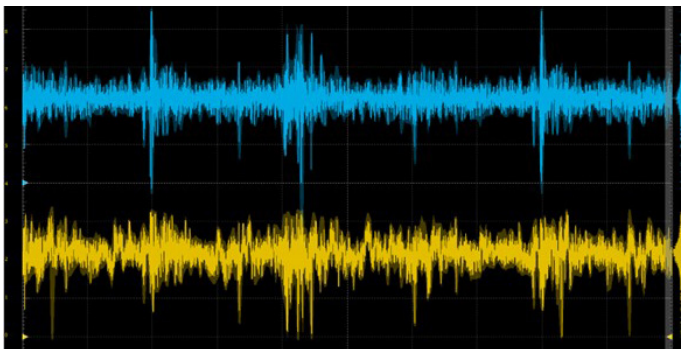

Fig. 18. Regular operation with embedded processing: original signal [blue] and filtered signal [yellow]. The horizontal axis represents time, while the vertical axis represents the amplitude in volts of the measured signal.

D. Results Analysis

Fig. 22 shows the signal-to-noise ratio of the DSP, sensor-computer-actuator, and embedded systems. This measure analyzes the filtering quality of the signals by removing a noise signal, which is a white noise type generated artificially. Both the convergence points of the embedded processing system and the sensor-computer-actuator system are highlighted -the convergence delay is also depicted for the latter-.

Table I shows the comparative results of the filtering paradigms. The fastest processing system is the sensor-computer-actuator system. In contrast, the embedded system exhibits processing times close to those of the distributed system, and the classic DSP system is considerably slower than the others. The mean shift in the sensor-computer-actuator and embedded processing systems is minimal. Meanwhile, the classical DSP system strongly changes the signal's nature, which is evident from the mean shift. The only filtering system that does not come into action when the system is turned on is the sensor-computer-actuator system, which needs a calibration and algorithm adaptation time.

Regarding the use of resources, the best is the DSP system, as it needs only one signal source, the SEMG acquisition source. However, in addition to the SEMG signal source, sensor-computer-actuator

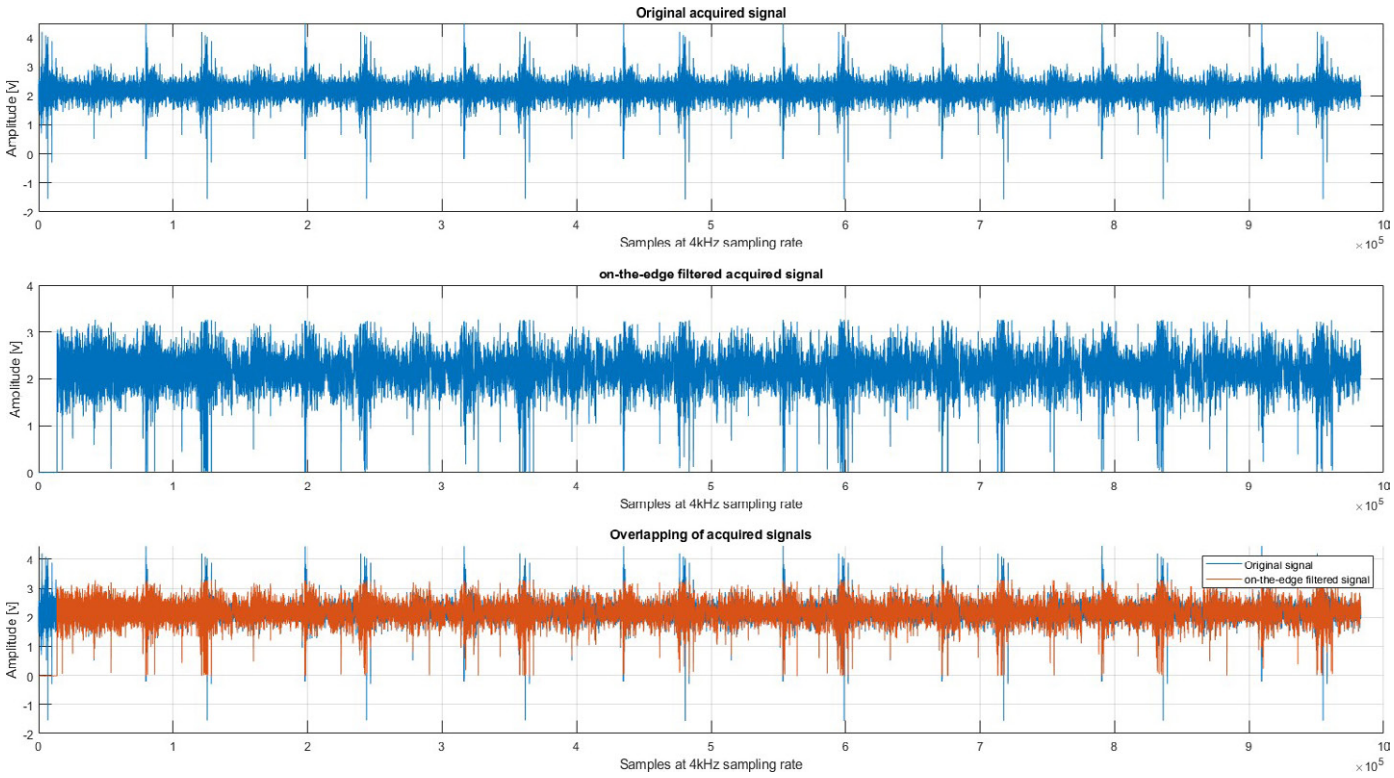

Fig. 19. Original signal vs filtered signal using an embedded system.

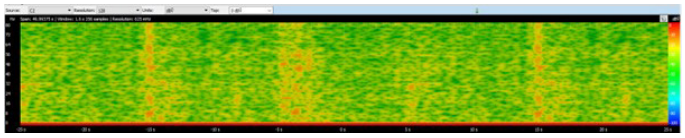

Fig. 20. Embedded processing-driven spectrogram of the original signal. The horizontal axis represents time, while the vertical axis represents the frequency in Hz of the measured signal. Source.

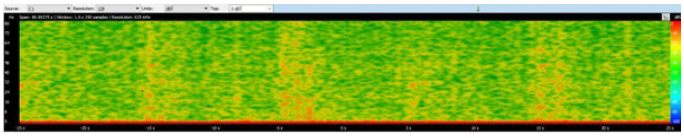

Fig. 21. Embedded processing-driven spectrogram of filtered signal. The horizontal axis represents time, while the vertical axis represents the frequency in Hz of the measured signal Source.

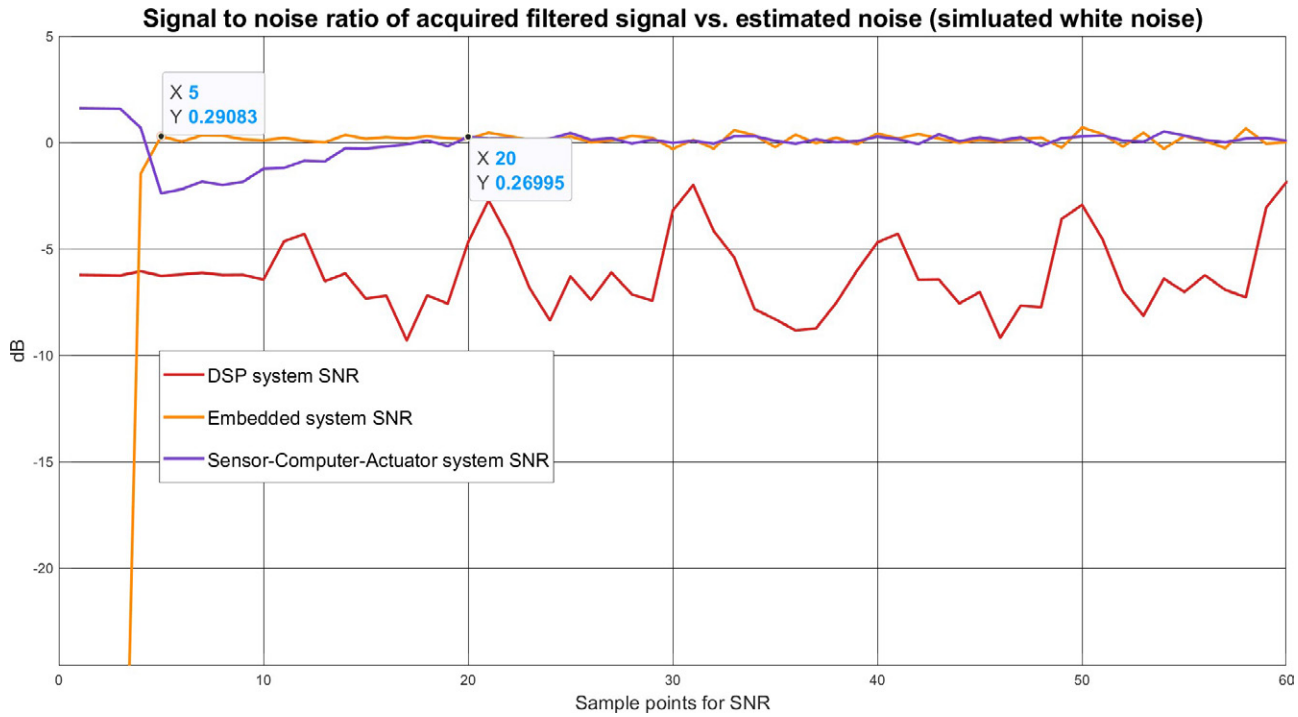

Fig. 22. SNR comparison of analyzed signals. In red is the SNR of the DSP system, in orange is the SNR of the embedded system, and in purple is the SNR of the sensor-computer-actuator system.

TABLE I. Comparative Results of Filtering Paradigms

	DSP	Sensor - Computer - Actuator	Embedded System
Processing Time	36.43 ms	2.573 ms	3.822 ms
Mean Shift	1.248 V	18 mV	19 mV
Immediate Action	Yes	No	Yes
Resources	One signal source	Two signal sorurces, network interface, PC	Two signal sources
SNR Mean	-6.321 db	0.11124 dB	0.15125 dB

and embedded processing systems need a second signal source to acquire noise. Therefore, the system that consumes the most physical resources is the distributed one, which requires a network interface and a high-capacity computer capable of executing the calculations involved in this processing.

The signal-to-noise ratio (SNR) determines the filtering quality, comparing the power of the filtered signal with the power of the noisy signal, which, in this case, is a simulated white noise signal. The results show that both the embedded processing and sensor-computer-actuator systems improve the signal, even if it is minimal. Meanwhile, the traditional DSP system does not fulfill the task of eliminating this type of noise, resulting in an average SNR of -6,321 dB. Again, Fig. 22 shows that the convergence speed of the distributed computing system is lower than that of the on-the-edge system.

E. Discussion

The results and measurements presented in the previous sections show that, although the sensor-computer-actuator processing is the fastest, it is more unstable, generating losses of information when the buffers of the communication socket are saturated. In addition, it requires more hardware equipment due to implementing a wireless communication system based on Wi-Fi. An intermediary is needed in the network structure connected to the Internet, which affects the security of the transmitted data. Nevertheless, a computer with good characteristics can adequately perform all the calculation and communication processes.

Regarding the traditional DSP system, it is the most widely used to date because of the relative simplicity of its implementation and the fact that it does not require modeling or acquisition of the signal noise to be removed. These features allow the processing system to act on its own. Furthermore, the algorithms presented in this paper can be optimized using C language or even by building hardware modules in HDL that can be implemented in the FPGA part of the embedded system—radically accelerating the computational speed of the system.

Although the processing delay is about 70 % in the embedded processing system, it is still much faster than the traditional DSP processing system. It implies a good use of hardware and software resources with the great advantage of adaptability to the noise sources that a surface EMG signal may suffer, which may change over time in amplitude and nature.

The embedded processing methodology is the cheapest and most efficient online learning technique in terms of resources since it eliminates the entire network interface of the distributed system. It has an adequate processing time, much shorter than DSP (showing a significant improvement in this area) and slightly longer than the sensor-computer-actuator system. It allows immediate action in terms of processing while reducing the external computational load that can be a problem when dealing with EMG signals.

V. Final Remarks

The processing and filtering of EMG signals are crucial for using these signals in prosthetic-device control processes or medical diagnostics. Traditionally, rigid filtering structures based on DSP have been used, although it does not acknowledge the non-LTI characteristics of the EMG. Subsequently, for more complex processes respecting the intrinsic characteristics of the system, all the information to be processed is sent to a discrete computing unit with which they usually communicate wirelessly. Therefore, addressing an integral processing methodology embedded in the device is appropriate because of the technological advances in the miniaturization of silicon processing systems and their increased computational capacity. Furthermore, embedded processing implies that the intelligent processing algorithms and decision-making are implemented on-device, eliminating discrete computing systems and substantially improving the processing that traditional LTI DSP techniques offer.

Objective comparison is made between the traditional DSP system, the discrete processing system, and the embedded processing system using the same device and the same database reconstructed by a function generator. The spectrograms of the signals, the delays due to the processing, and the signal-to-noise ratio are evaluated. The intelligent filtering algorithm is an adaptive RLS filter to which a simulated white noise signal is introduced as a noise source.

It was not found in the literature review any contribution to the implementation of adaptive filters for sEMG in an embedded system. Most of them use distributed computation systems in MATLAB. The most significant contribution of this paper is introducing a real-time implementation of adaptive filtering algorithms respecting the non-LTI characteristics of the EMG signals.

Given the current technological availability, it is appropriate and even advisable to perform intelligent data processing on-device. Even if a distributed processing system is still necessary for further processing, embedding processing blocks is advisable. It will reduce the computational load by receiving helpful information and not only raw data. Embedding intelligent processing blocks in the acquisition device will allow building more complex processing architectures and signal usage techniques, offering better results to end-users.

Therefore, intelligent embedded (edge AI) processing of electromyographic signals is more effective than traditional hardware processing. Embedding the processing is more effective because the time delay between signals is shorter than in a sensor-computer-actuator system. Suppose the noise interfering with the desired signal is properly characterized or acquired with secondary sensors. In that case, it can provide highly relevant information without considerable changes in the frequency and temporal nature of the electromyographic signals. On the other hand, considering the current state of technology, applying embedded artificial intelligence techniques is justified since they reduce the computational load suffered by other devices and allow the development of architectures with greater scalability. Furthermore, the autonomy of processing between the intelligent nodes that make up an acquisition system can be considered relevant. Even the total autonomy of each sensor is possible and does not require an auxiliary computing system or auxiliary conditioning of the signals to carry out the decision-making process.

Acknowledgments

The authors acknowledges the valuable support given by the SDAS Research Group (https://sdas-group.com/ –Accesed on: 11-Jul-2022).

References

[1] R. M. Rangayyan, *Biomedical Signal Analysis*. IEEE Press, 2nd ed., 2015.

[2] R. Singh, N. Rajpal, R. Mehta, "An empiric analysis of wavelet-based feature extraction on deep learning and machine learning algorithms for arrhythmia classification," *International Journal of Interactive Multimedia and Artificial Intelligence*, 2021, doi: 10.9781/ijimai.2020.11.005.

[3] C. Li, G. Li, G. Jiang, D. Chen, H. Liu, "Surface emg data aggregation processing for intelligent prosthetic action recognition," *Neural Computing and Applications*, vol. 32, pp. 16795–16806, 11 2020, doi: 10.1007/S00521- 018-3909-Z/TABLES/4.

[4] G. Li, O. W. Samuel, C. Lin, M. G. Asogbon, P. Fang, P. O. Idowu, "Realizing efficient emg-based prosthetic control strategy," *Advances in Experimental Medicine and Biology*, vol. 1101, pp. 149–166, 2019, doi: 10.1007/978- 981-13-2050-7_6.

[5] D. Proaño-Guevara, J. Procel-Feijóo, J. Zhingre- Balcazar, L. Serpa-Andrade, "Biomimetical arm prosthesis: A new proposal," vol. 590, 2018, pp. 549– 558, Springer International Publishing.

[6] L. Resnik, H. H. Huang, A. Winslow, D. L. Crouch, Zhang, N. Wolk, "Evaluation of emg pattern recognition for upper limb prosthesis control: A case study in comparison with direct myoelectric control," *Journal of NeuroEngineering and Rehabilitation*, vol. 15, pp. 1–13, 3 2018, doi: 10.1186/S12984-018-0361- 3/FIGURES/3.

[7] J. Ribeiro, F. Mota, T. Cavalcante, I. Nogueira, V. Gondim, V. Albuquerque, A. Alexandria, "Analysis of man-machine interfaces in upper-limb prosthesis: A review," *Robotics 2019, Vol. 8, Page 16*, vol. 8, p. 16, 2 2019, doi: 10.3390/ROBOTICS8010016.

[8] Y. Li, J. Deng, Q. Wu, Y. Wang, "Eye-tracking signals based affective classification employing deep gradient convolutional neural networks," *International Journal of Interactive Multimedia and Artificial Intelligence*, vol. 7, 2021, doi: 10.9781/ijimai.2021.06.002.

[9] J. M. Fajardo, O. Gomez, F. Prieto, "Emg hand gesture classification using handcrafted and deep features," *Biomedical Signal Processing and Control*, vol. 63, p. 102210, 1 2021, doi: 10.1016/J.BSPC.2020.102210.

[10] J. V. Basmajian, C. J. D. Luca, *Muscles alive : their functions revealed by electromyography*. Williams & Wilkins, 1985.

[11] P. Konrad, *The abc of emg*. 2005.

[12] C. Tepe, M. C. Demir, "The effects of the number of channels and gyroscopic data on the classification performance in emg data acquired by myo armband," *Journal of Computational Science*, vol. 51, p. 101348, 4 2021, doi: 10.1016/J.JOCS.2021.101348.

[13] J. Kimura, *Electrodiagnosis in Diseases of Nerve and Muscle: Principles and Practice*. Oxford University Press, 4 ed., 2013.

[14] R. Merletti, D. Farina, *Surface Electromyography: Physiology, Engineering and Applications*. Wiley-IEEE Press, 4 2016.

[15] S. Cerutti, C. Marchesi, *Advanced Methods of Biomedical Signal Processing*. IEEE Press, 2011.

[16] K. A. Wheeler, H. Shimada, D. K. Kumar, S. P. Arjunan, "A semg model with experimentally based simulation parameters," *2010 Annual International Conference of the IEEE Engineering in Medicine and Biology Society, EMBC'10*, pp. 4258–4261, 2010, doi: 10.1109/IEMBS.2010.5627175.

[17] K. L. Moore, A. F. Dalley, A. M. R. Agur, *Clinically oriented anatomy*. Wolters Kluwer Health/Lippincott Williams & Wilkins, 2014.

[18] M. Yaserifar, A. S. Oliveira, "Surface emg variability while running on grass, concrete and treadmill," *Journal of Electromyography and Kinesiology*, vol. 62, p. 102624, 2 2022, doi: 10.1016/J.JELEKIN.2021.102624.

[19] J. W. Lee, M. J. Shin, M. H. Jang, W. B. Jeong, S. J. Ahn, "Two-stage binary classifier for neuromuscular disorders using surface electromyography feature extraction and selection," *Medical Engineering & Physics*, vol. 98, pp. 65–72, 12 2021, doi: 10.1016/J.MEDENGPHY.2021.10.012.

[20] T. Lulic-Kuryllo, F. Negro, N. Jiang, C. R. Dickerson, "Standard bipolar surface emg estimations mischaracterize pectoralis major activity in commonly performed tasks," *Journal of Electromyography and Kinesiology*, vol. 56, p. 102509, 2 2021, doi: 10.1016/J.JELEKIN.2020.102509.

[21] M. M. Yassin, A. M. Saber, M. N. Saad, A. M. Said, A. M. Khalifa, "Developing a low-cost, smart, handheld electromyography biofeedback system for telerehabilitation with clinical evaluation," *Medicine in Novel Technology and Devices*, vol. 10, p. 100056, 6 2021, doi: 10.1016/J.MEDNTD.2020.100056.

[22] L. E. Sánchez-Velasco, M. Arias-Montiel, E. Guzmán- Ramírez, E. Lugo-González, "A low-cost emg- controlled anthropomorphic robotic hand for power and precision grasp," *Biocybernetics and Biomedical Engineering*, vol. 40, pp. 221–237, 1 2020, doi: 10.1016/J.BBE.2019.10.002.

[23] E. Noboa, M. Rácz, L. Szucs, P. Galambos, G. Márton, Eigner, "Development of an emg based svm supported control solution for the platypous education mobile robot using mindrove headset," *IFAC-PapersOnLine*, vol. 54, pp. 304–309, 1 2021, doi: 10.1016/J.IFACOL.2021.10.273.

[24] H. J. Hermens, B. Freriks, C. Disselhorst-Klug, G. Rau, "Development of recommendations for semg sensors and sensor placement procedures," *Journal of Electromyography and Kinesiology*, vol. 10, pp. 361–374, 10 2000, doi: 10.1016/S1050-6411(00)00027-4.

[25] D. Stegeman, H. Hermens, "Standards for surface electromyography: The european project surface emg for non-invasive assessment of muscles (seniam)," *SENIAM*, pp. 108–112, 2007.

[26] A. Pashaei, M. R. Yazdchi, H. R. Marateb, "Designing a low-noise, high-resolution, and portable four channel acquisition system for recording surface electromyographic signal.," *Journal of medical signals and sensors*, vol. 5, pp. 245–52, 2015.

[27] T. Roland, S. Amsuess, M. F. Russold, W. Baumgartner, "Ultra-low-power digital filtering for insulated emg sensing," *Sensors (Switzerland)*, vol. 19, pp. 1–24, 2019, doi: 10.3390/s19040959.

[28] L. Rozaqi, A. Nugroho, K. H. Sanjaya, A. I. Simbolon, "Design of analog and digital filter of electromyography," *Proceeding - 2019 International Conference on Sustainable Energy Engineering and Application: Innovative Technology Toward Energy Resilience, ICSEEA 2019*, pp. 186–192, 2019, doi: 10.1109/ICSEEA47812.2019.8938645.

[29] A. K. Sahu, A. K. Sahu, "A review on different filter design techniques and topologies for bio- potential signal acquisition systems," *Proceedings of the 3rd International Conference on Communication and Electronics Systems, ICCES 2018*, pp. 934–937, 2018, doi: 10.1109/CESYS.2018.8723912.

[30] H. Tankisi, D. Burke, L. Cui, M. de Carvalho, S. Kuwabara, S. D. Nandedkar, S. Rutkove, E. Stålberg, M. J. van Putten, A. Fuglsang-Frederiksen, "Standards of instrumentation of emg," *Clinical Neurophysiology*, vol. 131, pp. 243–258, 2020, doi: 10.1016/j.clinph.2019.07.025.

[31] S. W. Smith, *The scientist and engineer's guide to digital signal processing*. California Technical Publishing, 2nd ed., 1997.

[32] A. Oppenheim, R. Schafer, J. Buck, *Discrete-Time Signal Processing*. Prentice Hall Press, 2nd ed., 1998.

[33] R. Woods, J. McAllister, G. Lightbody, Y. Yi, *FPGA- Based Implementation of Signal Processing Systems*. Wiley, 10 2008.

[34] A. Viveros-Melo, L. Lasso-Arciniegas, J. A. Salazar- Castro, D. H. Peluffo-Ordóñez, M. A. Becerra, A. E. Castro-Ospina, E. J. Revelo-Fuelagán, "Exploration of Characterization and Classification Techniques for Movement Identification from EMG Signals: Preliminary Results," in *Communications in Computer and Information Science*, 2018, pp. 139–149, doi: 10.1007/978-3-319-98998-3_11.

[35] L. Lasso-Arciniegas, A. Viveros-Melo, J. A. Salazar- Castro, M. A. Becerra, A. E. Castro-Ospina, E. J. Revelo-Fuelagán, D. H. Peluffo-Ordóñez, "Movement Identification in EMG Signals Using Machine Learning: A Comparative Study," in *Lecture Notes in Computer Science (including subseries Lecture Notes in Artificial Intelligence and Lecture Notes in Bioinformatics)*, 2018, pp. 368–375, doi: 10.1007/978-3-030-01132-1_42.

[36] S. Haykin, B. Kosko, *Intelligent Signal Processing*. IEEE Press, 12 2001.

[37] C. S. Palacios, S. L. Romero, "Calibración automática en filtros adaptativos para el procesamiento de señales emg," *Revista Iberoamericana de Automatica e Informatica Industrial*, vol. 16, pp. 1–6, 2011.

[38] I. F. Ghalyan, Z. M. Abouelenin, V. Kapila, "Gaussian filtering of emg signals for improved hand gesture classification," *2018 IEEE Signal Processing in Medicine and Biology Symposium, SPMB 2018 - Proceedings*, pp. 1– 6, 2019, doi: 10.1109/SPMB.2018.8615596.

[39] M. Z. Jamal, D. H. Lee, D. J. Hyun, "Real time adaptive filter based emg signal processing and instrumentation scheme for robust signal acquisition using dry emg electrodes," *2019 16th International Conference on Ubiquitous Robots, UR 2019*, pp. 683–688, 2019, doi: 10.1109/URAI.2019.8768662.

[40] S. Márquez-Figueroa, Y. S. Shmaliy, O. Ibarra- Manzano, "Optimal extraction of emg signal envelope and artifacts removal assuming colored measurement noise," *Biomedical Signal Processing and Control*, vol. 57, p. 101679, 2020, doi: 10.1016/j.bspc.2019.101679.

[41] L. L. Menegaldo, "Real-time muscle state estimation from emg signals

during isometric contractions using kalman filters," *Biological Cybernetics*, vol. 111, pp. 335– 346, 2017, doi: 10.1007/s00422-017-0724-z.

[42] P. Okoniewski, S. Kocon, J. Piskorowski, "Linear time-varying multi-notch fir filter for fast emg measurements," *2018 23rd International Conference on Methods and Models in Automation and Robotics, MMAR 2018*, pp. 634–637, 2018, doi: 10.1109/MMAR.2018.8486122.

[43] A. R. Verma, Y. Singh, B. Gupta, "Adaptive filtering method for emg signal using bounded range artificial bee colony algorithm," *Biomedical Engineering Letters*, vol. 8, pp. 231–238, 2018, doi: 10.1007/s13534-017-0056-x.

[44] T. Yu, K. Akhmadeev, E. L. Carpentier, Y. Aoustin, D. Farina, "On-line recursive decomposition of intramuscular emg signals using gpu-implemented bayesian filtering.," *IEEE transactions on bio-medical engineering*, 2019, doi: 10.1109/TBME.2019.2948397.

[45] P. S. R. Diniz, *Adaptive Filtering*. Springer US, 2008.

[46] M. Limem, M. A. Hamdi, M. A. Maaref, "Denoising uterine emg signals using lms and rls adaptive algorithms," 3 2016, pp. 273–276, IEEE.

[47] A. C. Mugdha, F. S. Rawnaque, M. U. Ahmed, "A study of recursive least squares (rls) adaptive filter algorithm in noise removal from ecg signals," 6 2015, pp. 1–6, IEEE.

[48] P. Singh, K. Bhole, A. Sharma, "Adaptive filtration techniques for impulsive noise removal from ecg," 12 2017, pp. 1–4, IEEE.

[49] M. R. Ahmed, R. Halder, M. Uddin, P. C. Mondal, A. K. Karmaker, "Prosthetic arm control using electromyography (emg) signal," *2018 International Conference on Advancement in Electrical and Electronic Engineering, ICAEEE 2018*, 2 2019, doi: 10.1109/ICAEEE.2018.8642968.

[50] K. T. Kim, S. Park, T. H. Lim, S. J. Lee, "Upper- limb electromyogram classification of reaching- to-grasping tasks based on convolutional neural networks for control of a prosthetic hand," *Frontiers in Neuroscience*, vol. 15, p. 1311, 10 2021, doi: 10.3389/FNINS.2021.733359/BIBTEX.

[51] G. M. Hägg, B. Melin, R. Kadefors, "Applications in ergonomics," 2005. doi: 10.1002/0471678384.ch13.

[52] Y. H. Hsueh, C. Yin, Y. H. Chen, "Hardware system for real-time emg signal acquisition and separation processing during electrical stimulation," *Journal of Medical Systems*, vol. 39, 2015, doi: 10.1007/s10916-015- 0267-6.

[53] D. Z. Yinfeng Fang, "Isrmyo-i: A database for semg- based hand gesture recognition," 2018. [Online]. Available: https://dx.doi.org/10.21227/H26Q26, doi: 10.21227/H26Q26.

[54] Y. Fang, H. Liu, G. Li, X. Zhu, "A multichannel surface EMG system for hand motion recognition," *International Journal of Humanoid Robotics*, vol. 12, p. 1550011, may 2015, doi: 10.1142/s0219843615500115.

[55] Q. Ai, Q. Liu, W. Meng, S. Q. Xie, "Neuromuscular signal acquisition and processing," in *Advanced Rehabilitative Technology*, Elsevier, 2018, pp. 33–66, doi: 10.1016/b978-0-12-814597-5.00003-5.

[56] M. Sharma, N. Gaddam, T. Umesh, A. Murthy, P. K. Ghosh, "A comparative study of different EMG features for acoustics-to-EMG mapping," in *Interspeech 2021*, aug 2021, ISCA.

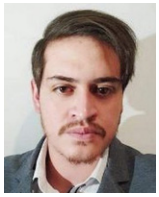

Daniel Proaño-Guevara

Daniel received his B.Eng. degree in electronics engineering from the Universidad Politécnica Salesiana, Ecuador, 2019, his M.Sc. in artificial intelligence from Universidad Internacional de La Rioja UNIR, Spain, 2020, and he is currently studying his M.Eng. in electronics engineering from the Instituto Superior Técnico-Universidade de Lisboa, Portugal. His research interest includes intelligent digital signal processing, artificial intelligence, embedded systems design, FPGA, and biomedical engineering. Currently, he is a research assistant at the SDAS group.

Xiomara Blanco Valencia

She is originally from Bogotá, Colombia; she studied for her System Engineering degree at the University of Santander in Bucaramanga and then moved to Salamanca, Spain, where she studied for her master's degree and PhD in Artificial Intelligence at the University of Salamanca. She is currently working as Professor at the Department of Computer Science at Universidad Internacional de La Rioja, Spain. In addition, she is a member of the Smart Data Analysis Systems Group SDAS Group. Her research interests include Artificial Intelligence, Soft computing, Recommender systems for health and Natural Language Processing.

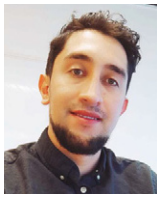

Paul D. Rosero-Montalvo

He is a Post. Doc at IT University of Copenhagen (ITU) in Denmark since June 2021. His research focuses on emerging microcontrollers to run machine learning models in decentralized networks. Earlier, He was a research assistant professor in the Applied Science Department at the Universidad Tecnica del Norte (UTN), Ecuador, for seven years. At the same time, he was a part-time lecturer in the TI Department at Instituto Tecnologico 17 de Julio, Ecuador. He received his Ph.D. from the University of Salamanca in Spain in November 2020, where Prof. Vivian Lopez-Batista advised him. He has a master's degree in Data Management systems from Universidad de las Fuerzas Armadas ESPE, Ecuador (2018), and an Engineering degree in Electronics and Telecommunications from UTN (2013).

Diego H. Peluffo-Ordóñez

He was born in Pasto - Colombia in 1986. He received his degree in electronic engineering, Master's in industrial automation and PhD in engineering from the Universidad Nacional de Colombia, Manizales - Colombia, in 2008, 2010 and 2013, respectively. In 2012, he undertook his doctoral internship at KU Leuven - Belgium.From 2013 to 2014, he worked as a post-doc at Université Catholique de Louvain at Louvain la-Neuve - Belgium. From 2014 to 2015, he worked as a lecturer at Universidad Cooperativa de Colombia - Pasto.From 2015 to 2017, he worked as a researcher/professor at Universidad Técnica del Norte - Ecuador. From 2017 to 2020, he worked as a researcher/professor at Yachay Tech - Ecuador. From 2020 to 2022, he worked as a Consultant/Curriculum Author at deeplearning.ai. Currently, he is working as an assistant professor at the Modeling, Simulation and Data Analysis (MSDA) Research Program from Mohammed VI Polytechnic University - Morocco. He works as a Master's thesis advisor with the Artificial Intelligence Master's program from Universidad Internacional de La Rioja (UNIR) - Spain. He is the founder and head of the SDAS Research Group. As well, he works as an invited lecturer and an external researcher at Corporación Universitaria Autónoma de Nariño - Pasto, Colombia, and is a member of SEDMATEC Research Group. Also, he is an external collaborator at Writing Lab from Tecnológico de Monterrey - Mexico. As well, he is an external supervisor of PhD programs at Universidad de Granada - Spain, Universitat Politècnica de València - Spain,and Universidad Nacional de La Plata - Argentina.He has served as an organizing committee member (general chair, session chair, competitions chair) as well as a keynote speaker in several conferences. Also, he has served as a guest editor for the Computers and Electrical Engineering Journal. His main research interests are kernel-based and spectral methods for data clustering and dimensionality reduction. The scope of his topics of interest encompasses complex high-dimensional data, signal, image and video analysis for medical and industry applications.